EVALUATION OF TECHNOLOGICAL RADIATION SOURCES IN THE PUMPING STATION OF THE PRIMARY CIRCULATION LOOP AND ON THE TOP OF THE POOL TYPE RESEARCH REACTOR

by

Stoyan H. KADALEV

College of Energy and Electronics, Technical University of Sofia, Sofia, Bulgaria

Scientific paper
http://doi.org/10.2298/NTRP1801031K

The present paper considers the approach to an assessment of technological radiation sources in the primary water-water reactor circulation loop. In principle, such an evaluation is a multidisciplinary task that covers not only the irradiation of the nuclei, the formation of new isotopes and their decay when they are unstable, but also calculations in the field of hydraulics in order to perform an assessment of the irradiation time and the decay time. A general and a more detailed review of the radiation sources formation in the nuclear facilities and the pool type research reactors with demineralized water as a heat carrier are prepared. The initial isotopic composition of the heat carrier has been adopted according to the Vienna Standard Mean Ocean Water recommended by the International Atomic Energy Agency.
The general mathematical model of the processes of nuclei irradiation, the formation of new isotopes and their decay, the assessment of the irradiation time and the decay time is described in details, enabling the repetition of this evaluation to a particular facility. The presented approach is applied in the reconstruction design of the nuclear research reactor IRT-2000, Sofia, Bulgaria.

Key words: induced radiation, heat carrier activation, technological radiation source

INTRODUCTION

The main source of ionizing radiation in most nuclear facilities is the reactor core. The ionizing radiation sources in the primary circulation loop are fission products which could leak into the coolant from the fuel on account of defects and/or damages in the fuel elements cladding activated elements of the heat carrier and its impurities and activated corrosion products of the structural materials [1]. Other ionizing radiation sources are the storage pools for irradiated fuel, the equipment of the water treatment systems, the ventilation systems, *etc*.

The pool type research reactors are usually water cooled, water moderated, with two coolant loops, so the present study covers the peculiarities of this type of reactors.

The safety analyses report (SAR) scope of the research reactor includes the assessment of the radiation situation in the premises of the primary circulation loop pumping station and on the top of the reactor at normal operation and in emergency situations. The induced activity of the heat carrier in the primary circulation loop has a significant share in the radiation situation at these places. It consists of the coolant activity and the activity of its impurities. The impurities consist of technological impurities, products of corrosion and fission products leaked in the coolant due to the damaged fuel elements.

It is assumed that the fission products enter the coolant only from the fuel elements with damaged cladding, which is considered as an emergency situation.

The presence of radioactive corrosion products in the technological loop is due to the following processes:

- the activation of the structural materials under the direct irradiation with subsequent corrosion and entering of its products in the coolant,
- the activation of the stable nuclei in the corrosion products due to the irradiation during the coolant passage through the core, and
- the activation of the stable nuclei in the corrosion products during their sedimentation on the structures surface in the irradiation area.

The peculiarity of pool type research reactors is the use of demineralized water as a heat carrier, aluminum alloys as basic constructional material of the primary circulation loop and internal pool devices and stainless steel piping between the pool and the primary

* Corresponding author; e-mail: stojan.kadalev@gmail.com

circulation loop pumping station, making the availability of products of corrosion a negligible value.

An additional factor in the radiation situation on the top of the reactor is the presence of ionizing radiation sources for dosimetry equipment calibration and irradiated samples in the vertical experimental channels. The contribution in the common radiation background of these sources is considered separately in the radiation situation assessment of the relevant activities safety analysis.

Based on the foregoing, the present study covers only the heat carrier activity caused by the irradiation of the nuclei of the water molecule elements.

GENERAL DESCRIPTION OF THE TASK

The subject of the presented study is the impact assessment on the radiation situation in two control points. The first point is the pumping station premises of the primary circulation loop, in which the pipes and the heat exchanger are examined as a linear radiation source. The second control point is a volumetric radiation source in the reactor pool on the outlet level of the grid of the ejector system vessel with the following dimensions: the height and the width of the grid and a length equal to the distance between the grid and the point above the center of the reactor core. The evaluation purpose is providing the data for the subsequent assessment of the radiation situation in the pumping station premises and on the top of the reactor at normal operating conditions. As the only source of secondary radiation on the specified locations, the isotopic composition of water is discussed in more detail.

The isotopes content of hydrogen and oxygen in natural waters is defined by the international standards set by the International Atomic Energy Agency (IAEA):

The standard – Vienna Standard Mean Ocean Water (VSMOW) determines the isotopic composition of the world ocean water.

The standard – Standard Light Antarctic Precipitation (SLAP) determines the isotopic composition of the natural water in Antarctica.

The standard – Greenland Ice Sheet Precipitation (GISP) determines the isotopic composition of the natural water in Greenland.

It is apparent that the present study should be guided by the data in the VSMOW standard, presented in tab. 1 [2].

As a result of the water nuclei irradiation, new isotopes are obtained. They are presented in tab. 2 [1, 3-5].

The transformation chain and the decay chain of the obtained isotopes are as follows

$$ {}^{1}_{0}n \quad {}^{16}_{8}O \quad {}^{1}_{1}p \quad {}^{16}_{7}N \quad {}^{16}_{7}N \quad \beta, \gamma \quad {}^{16}_{8}O \qquad \text{Number (1)} $$

Table 1. The isotope content of water according to the VSMOW standard

Position number	Water isotopologue	Molecular mass [u]	Contents [gkg^{-1}]	Contents [%]
1	$^{1}H_2{}^{16}O$	18,01056470	997,032536356	99,7032536356
2	$^{1}H^{2}H^{16}O$	19,01684144	0,328000097	0,0328000097
3	$^{2}H^{16}O$	20,02311819	0,000026900	0,0000026900
4	$^{1}H_2{}^{17}O$	19,01478127	0,411509070	0,0411509070
5	$^{1}H^{2}H^{17}O$	20,02105801	0,000134998	0,0000134998
6	$^{2}H^{17}O$	21,02733476	0,000000011	0,0000000011
7	$^{1}H_2{}^{18}O$	20,01481037	2,227063738	0,2227063738
8	$^{1}H^{2}H^{18}O$	21,02108711	0,000728769	0,0000728769
9	$^{2}H_2{}^{18}O$	22,02736386	0,000000059	0,0000000059

Table 2. Activation reactions and properties of the obtained isotopes

Number	Activation reaction	Microscopic cross-section for activation, σ_a [10^{24} cm^2]	Half-life of the obtained isotope, $T_{½}$
1	$^{16}O(n, p)^{16}N$	1.90 10^{-5}	7.13 s
2	$^{17}O\ (n, p)\ ^{17}N$	5.30 10^{-6}	4.14 s
3	$^{18}O\ (n, p)\ ^{18}F$	8.00 10^{-6}	109.77 min
4	$^{18}O\ (n, \gamma)\ ^{19}O$	1.60 10^{-6}	26.91 s
5	$^{2}H\ (n, \gamma)\ ^{3}H$	5.19 10^{-4}	12.33 year

The presented cross-sections of the radiative capture reactions (n, γ) are for the energy range of thermal neutrons; the other cross-sections are averaged on the fission neutrons spectrum

$$ {}^{1}_{0}n \quad {}^{17}_{8}O \quad {}^{1}_{1}p \quad {}^{17}_{7}N \quad {}^{17}_{7}N \quad \beta, n \quad {}^{16}_{8}O \qquad \text{Number (2)} $$

$$ {}^{1}_{0}n \quad {}^{18}_{8}O \quad {}^{1}_{1}p \quad {}^{18}_{9}F \quad {}^{18}_{9}F \quad \beta, \gamma \quad {}^{18}_{8}O \qquad \text{Number (3)} $$

$$ {}^{1}_{0}n \quad {}^{18}_{8}O \quad \gamma \quad {}^{19}_{8}O \quad {}^{19}_{8}O \quad \beta, \gamma \quad {}^{19}_{9}F \qquad \text{Number (4)} $$

$$ {}^{1}_{0}n \quad {}^{2}_{1}H \quad \gamma \quad {}^{3}_{1}H \quad {}^{3}_{7}H \quad \beta \quad {}^{2}_{2}He \qquad \text{Number (5)} $$

Based on the provided information, the accumulation of radioactive isotopes in the control points is assessed.

It is apparent that some of the water isotopologues are contained in relatively small amounts in natural composition. The following criterion is accepted as a first step for the study simplification: the respective isotopologue is negligible if its content is less than 10^{-4} %. As a second simplification step, it is accepted that only the isotopes with electrically neutral emanation will be examined. Given these criteria the present study covers the oxygen nuclei of the isotopologues presented in tab. 1 on positions 1, 2, 4, and 7.

MATHEMATICAL MODELING OF THE PROCESSES

The mathematical model for calculating the coolant activity depends on the reactor cooling technological scheme [1, 4, 6]. In the simplest case, with a single-phase coolant without the contour branches, leaks and filtration system, the specific activity of the isotope i is calculated using the formula

$$a_k^i \quad Y^i(1 \quad e^{\lambda^i\tau})\frac{1 \quad e^{(k \quad 1)\lambda^i t}}{1 \quad e^{\lambda^i t}}e^{\lambda^i t} \qquad (1)$$

where a_k^i [Bql^{-1}] is the specific activity of the isotope i in the coolant after k number of circulation cycles, Y^i – the integral of the nuclide predecessor activation of isotope i in the coolant, λ^i [s^{-1}] – the decay constant of isotope i, τ [s] – the irradiation duration of the coolant in the reactor core, k – the number of the heat carrier circulation cycles in the coolant loop, t [s] – the duration of the circulation cycle, and t`[s] – the heat carrier run time from the reactor core to the control point.

The integral of the activation Y^i determines the formation rate of isotope i per unit volume of the coolant in the reactor core

$$Y^i \quad \int_0^{E_n} \varphi(E_n)\,{}_a^i(E_n)\mathrm{d}E_n \qquad (2)$$

where $\varphi(E_n)$ [cm^{-2}s^{-1}] is the averaged over the coolant volume neutron flux with energy E_n, ${}_a^i(E_n)$ [cm^{-1}] – the macroscopic cross-section of the nuclide predecessor activation of isotope i upon irradiation with neutrons with energy E_n.

The macroscopic cross-section of the nuclide predecessor activation is calculated using the formula

$${}_a^i(E_n) \quad \rho_i\sigma_i(E_n) \qquad (3)$$

where ρ_i [cm^{-3}] is the nuclear density of the nuclide predecessor of isotope i, $\sigma_i(E_n)$ [cm^{-2}] – the microscopic cross-section of the nuclide predecessor activation of isotope i upon irradiation with neutrons with energy E_n, 10^{24}.

The nuclear density of the nuclide predecessor of isotope i is calculated using the formula

$$\rho_i \quad \frac{N_A\gamma_s}{M_s}n_i x_i \qquad (4)$$

where $N_A = 6.02214086\ 10^{23}$ mol^{-1} – the Avogadro's number, γ_s [gcm^{-3}] – the density of the substance, M_s [u] – the atomic mass of the substance, n_i – the number of atoms of the nuclide predecessor of isotope i in the substance molecule, and x_i – the isotopologue content in the substance.

If the technological scheme bifurcates, the presented model is complicated because of the need to consider the duration of the coolant movement through every section, the neutron flux on the relevant section (if the branch is in the reactor core), *etc*.

As a rule, the coolant of pool type reactors is single-phase and, therefore, a variant of the mathematical modeling of two-phase coolant is not considered.

The presented aspects of the mathematical modeling of the task show that its solution could be only the result of a multi disciplinary approach to the problem. The solution includes neutron-physical calculations of the reactor core, hydraulic calculations of the loop to determine the irradiation duration of the nuclide's predecessors, their activation and the decay time in the checkpoints.

At normal operation the coolant flow rate is constant and its velocity varies depending on the open flow area of the loop section. Under certain loop geometric parameters, the velocity values of the coolant and the passage time through each section and the contour as a whole can be defined.

The reactor core is adopted as the first of the considered sections. The average coolant velocity through the reactor core is defined by the formula [7]

$$v_{RC} \quad \frac{G}{S_{RC}} \qquad (5)$$

where v_{RC} [ms^{-1}] is the coolant velocity through the reactor core, G [m^{3}s^{-1}] – the flow rate of the coolant, and S_{RC} [m^2] – the open flow area of the reactor core.

After the coolant velocity through the reactor core is obtained, the irradiation time τ is calculated

$$\tau \quad \frac{l_{fm}}{v_{RC}} \qquad (6)$$

where l_{fm} [m] is the length of the fuel section.

In the next sections the velocity values are changing on the following relation [7]

$$v_n \quad \frac{v_{n\ 1}S_{n\ 1}}{S_n} \qquad (7)$$

where v_n [ms^{-1}] is the coolant velocity in section n, v_{n-1} [ms^{-1}] – the coolant velocity in section $n-1$, S_n [m^2] – the open flow area of section n, and S_{n-1} [m^2] – the open flow area of section $n-1$.

The movement duration through the section is defined by the formula

$$t_n \quad \frac{I_n}{v_n} \qquad (8)$$

where t_n [s] is the movement duration trough the section n, l_n [m] – the length of the section n, and v_n [ms^{-1}] – the coolant velocity in the section n.

After the coolant velocities and the coolant movement duration for each section are determined, the irradiation time τ of the coolant in the reactor core, the decay time t`in the control points and the circulation cycle duration t can be calculated.

The presented mathematical model was applied in the evaluation of the radiation situation in the pumping station of the primary circulation loop and on the top of the reactor in the design for the reconstruction of the research reactor IRT – 2000 and the calculation results are presented in the SAR of the facility.

GENERAL DESCRIPTION OF THE RECONSTRUCTION DESIGN OF IRT-2000 RESEARCH REACTOR

The research reactor IRT-2000 is the heterogeneous thermal neutron water-water pool type reactor, whose characteristics are retained in the reconstruction design, briefly presented in [8].

The distilled water is used as a coolant in order to protect the aluminum parts of the internal devices from corrosion and to minimize the radioactive content in the primary circulation loop. According to the design, the reactor core vessel (fig. 1) has a parallelepiped shape and dimensions 676 640 950 mm. The base of the vessel is a support plate with 54 cells with a pitch of 71.5 mm for attachment of fuel assemblies or reflective blocks. The coolant flows through the reactor core from top downwards with a flow rate up to 382 m^3h^{-1}, depending on the operation mode. The temperature at the outlet of the reactor core will not exceed 50 °C.

The reactor is foreseen to operate with low enriched uranium (LEU) fuel assemblies of the IRT-4M type (fig. 2) with enrichment 19.7 % ^{235}U [10] and with thermal power up to 1000 kW. The fuel assembly (FA) consists of eight (fig. 3-A) or six (fig. 3-B) concentrically arranged tubular fuel elements with a square cross-section and rounded corners. Either a control rod (CR) or a vertical experimental channel is positioned in the central hole of a six tube FA. There are 4 eight tube and 12 six tube fuel assemblies, 23 solid beryllium blocks, 2 beryllium blocks with a hole for vertical experimental channels and one beryllium block with the automatic control rod. For better transfer of the neutron fluxes the design provides 3 pieces of aluminum blocks, each occupying 4 cells, filled with water and air cavity at the level of the horizontal experimental channels.

The reactor core configuration (fig. 4) was developed in collaboration with the scientists from the Russian Research Centre (RRC) "Kurchatov Institute".

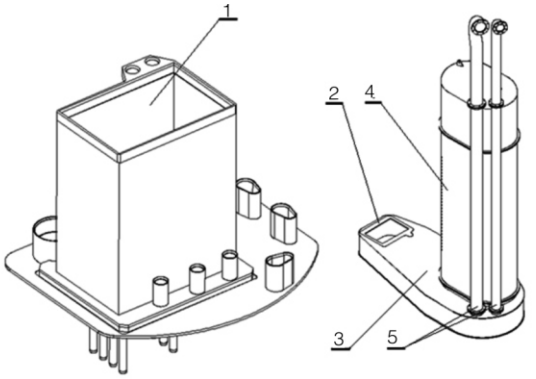

Figure 1.
1 – the reactor core vessel, 2 – the slot of the reactor core and the support plate, 3 – the delay tank, 4 – the ejector system vessel, 5 – the pipelines from and to the pump station of the primary circulation loop

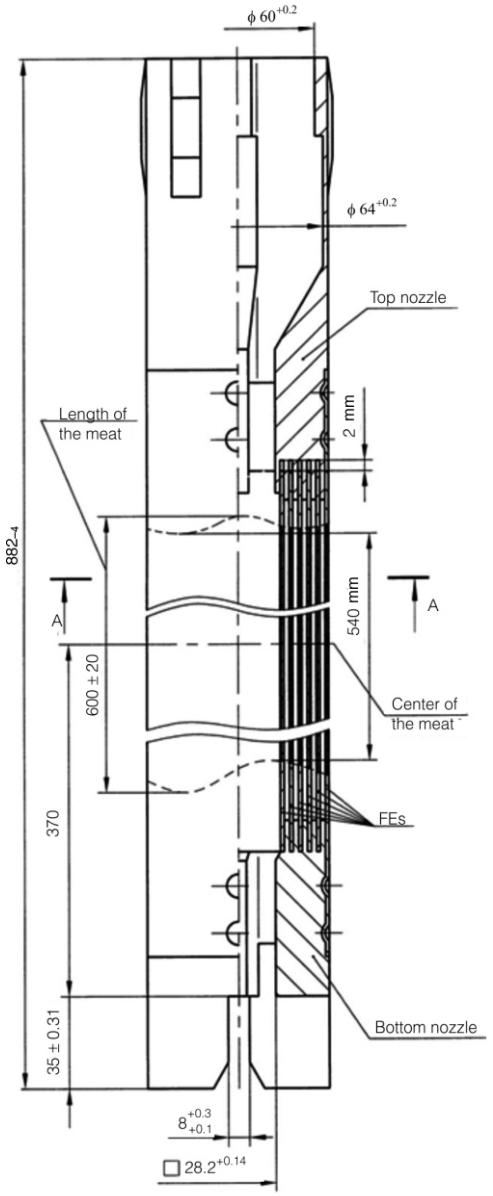

Figure 2. Fuel assembly type IRT-4M (all values are in mm)

The design provides the use of internal pool loop core cooling circuit, which (fig. 1), comprises of a delay tank designed to slow down the heat carrier speed after its departure from the core, in order to decrease the concentration of the short living isotope ^{16}N before the water enters in the pipes to the pump station of the primary circulation loop and the ejector system. The design provides that 37 % of the coolant flow through the reactor core passes through the pumps, the mechanical and ion exchange filters and the heat exchangers, where the reactor core heat is given away to the secondary circulation loop, and then the heat carrier returns to the pool through the ejector system nozzle.

According to the technological scheme (fig. 5) the primary circulation loop will be composed of two pumps, a filtration system with six filters – two me-

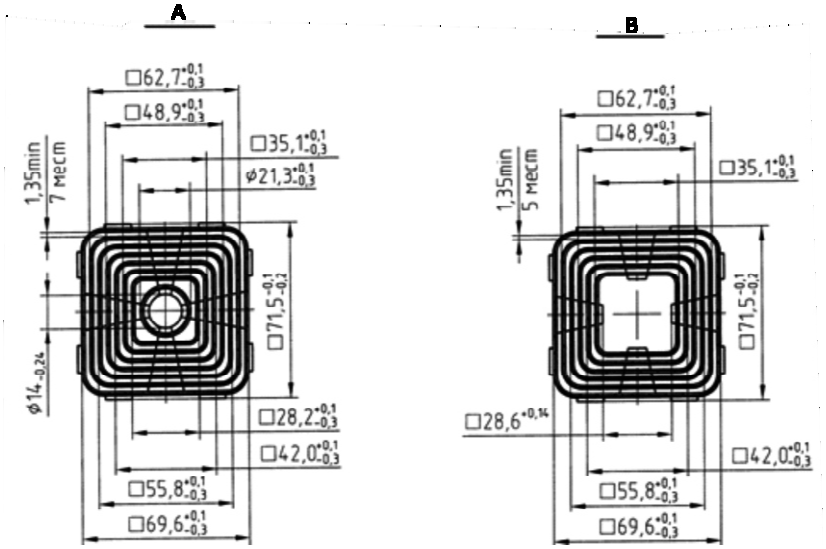

Figure 3. The cross-sections of 8-tube (A) and 6-tube (B) IRT-4M type FA (all values are in mm)
1 – fuel elements, 2 – the coolant channel, 3 – the control rod, 4 – the displacer tube

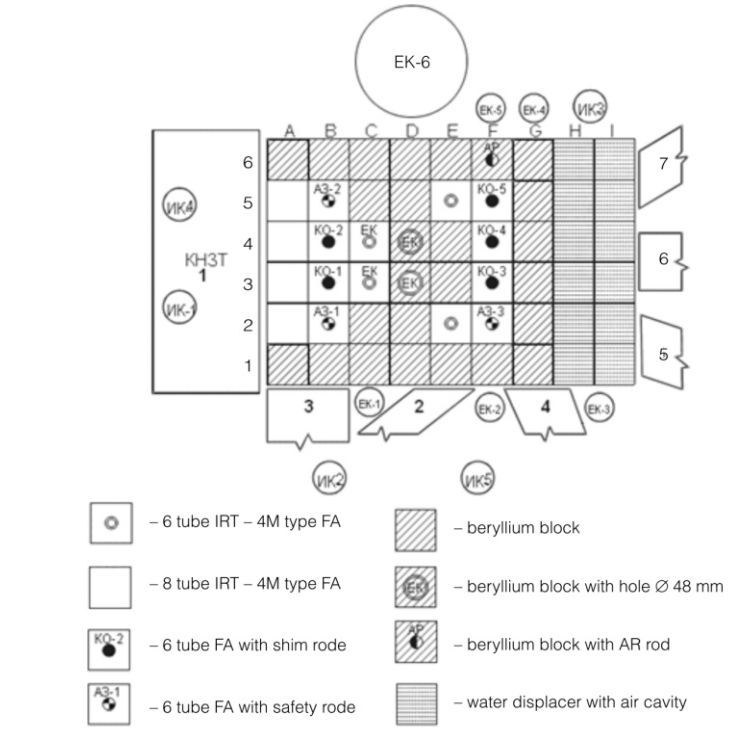

Figure 4. Reactor core configuration of IRT- 2000

chanical input and output filters and four ion exchange filters between them, and two heat exchangers. Secondary the circulation loop will consist of two pumps, two heat exchangers, which are common to circulation loops, nozzles and two spray ponds. The coolant in the secondary circulation loop is processed water.

INITIAL CONDITIONS AND CALCULATION AREAS

Definition of the initial conditions for the analysis

The calculations are made under the following assumptions:

- the reactor is in operation at power 200 kW,
- the maximum fuel meat length of the fuel elements is adopted according to the manufacturer documentation (B 0019.20.00.000 DKO) – 0.620 m (fig. 2),
- the calculations are made for the maximum neutron flux with the fission spectrum 1.391 10^{13} $cm^{-2}s^{-1}$,
- a constant neutron flux throughout the reactor core volume is assumed,
- one of the two pumps and one of the two heat exchangers on the primary circulation loop are in operation and the second pump and the second heat exchanger are standing in reserve, the flow rate G through the reactor core according to [9] is

$$G = 226\ m^3h^{-1} = 0.062778\ m^3s^{-1}$$

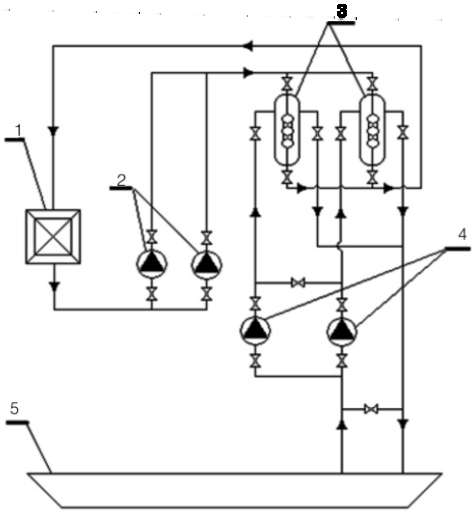

Figure 5. The technological scheme of IRT–2000
1 – the reactor core, 2 – the pump station of the primary circulation loop, 3 – the heat exchangers, 4 – the pump station of the secondary circulation loop, 5 – the spray ponds

- in order to achieve the maximum conservatism of the assessment, a combination of the technological equipment with the shortest heat carrier route from and to the reactor pool was chosen,
- a constant heat carrier pressure and temperature throughout the reactor core coolant circuit (internal and external pool cooling circuits) are assumed,
- in order to achieve the maximum conservatism of the assessment, the heat carrier flow mixing with the water in the pool volume after the grid of the ejector system vessel is not accounted for and the flow transition to a larger cross-section is assumed,
- to assess when the balance between the accumulation and the decay of the long-lived isotopes is achieved, an uninterrupted operation mode of the facility is adopted.

Definition of the calculation areas

In the design of the example facility a loop of the heat carrier flow is formed. The water penetrates from the pool into the reactor core (the irradiation area), passes through the delay tank, and enters the ejector system. At the entrance into the ejector system vessel (dividing point) the heat carrier flow divides in two parts. The first one (37 % of the heat carrier flow) enters into the conduit, passes through the pump station, heat exchangers, filter system and returns to the ejector system vessel through the ejector nozzle. The other part passes through the ejector vessel, surrounds the nozzle, goes into the confusor, wherein both parts are reunited and together go through the ejector system back into the pool through the grid in the housing of the ejector system vessel. In this way there is a by-pass of the pumping station, through which 63 % of the heat carrier passes.

In the so described contour the following major areas of the loop are highlighted:

- the first major area – the reactor core area (the irradiation and the decay time area),
- the second major area – the area between the reactor core and the entrance into the ejector system vessel, where the dividing point of the heat carrier is found (the decay time area),
- the third major area – the pumping station area, wherein 37 % of the heat carrier flow (Part A) passes through the external pool cooling circuit and returns through the nozzle, and the by-pass area, wherein 63 % (Part B) passes through the section between the entrance of the ejector system vessel and the nozzle, where the reunification point of the heat carrier is found (the decay time area),
- the fourth major area – from the ejector nozzle, wherein both heat carrier streams are reunited and mixed, to the grid of the ejector system vessel (a decay time area), and
- the fifth major area – after the grid of the ejector system vessel, wherein the heat carrier flow penetrates into the pool volume and reaches the reactor core entrance (a decay time area).

In some of the described areas there are also subareas which will be considered at the relevant stage.

CALCULATIONS

The calculations are carried out intwo main stages. In the first main stage, the irradiation duration of the heat carrier in the reactor core and the decay times at the dividing point, the reunification point and control points are calculated. In the second main stage, the number of circulation cycles needed to reach the equilibrium of the isotopes concentrations, the separate and summary isotopes concentrations in the control points, as well as at the reactor core inlet, are calculated.

First major area

The first step in determining the heat carrier velocity in the reactor core is calculating its open flow area S_{RC} which is the sum of the open flow areas of the elements and the housing of the reactor core. The results are presented in tab. 3.

Table 3. Geometrical parameters of the components in the reactor core

Component	Pcs.	S_n [mm^2]	ΣS_n [mm^2]
Six tubes fuel assembly	12	2492.9530	29915.4
Eight tubes fuel assembly	4	2857.8876	11431.6
Internal beryllium block	6	351.2500	2107.5
External beryllium block	13	351.2500	4566.3
Corner beryllium block	4	351.2500	1405.0
Beryllium block with CR	1	991.8400	991.8
Beryllium block with a hole	2	2159.8900	4319.8
Reactor core housing	1	–	–
S_{RC} [mm^2]	–	–	54737.4

According to eq. (5) with such a debit, the heat carrier velocity v_{RC} is

$$v_{RC} \quad \frac{G}{S_{RC}} \quad \frac{0.062778}{0.054737} \quad 1.147\ \text{m s}^{-1}$$

For the length of the fuel meat $l_{fm} = 0.620$ m according to eq. (6) the duration of the irradiation τ is

$$\tau \quad \frac{l_{fm}}{v_{RC}} \quad \frac{0.620}{1.147} \quad 0.54\ \text{s}$$

For the tang length of the fuel assembly $l_t = 0.095$ m according to eq. (7), the decay time t_1 in the first main area in the reactor core after the fuel meat is

$$t_1 \quad \frac{l_t}{v_{RC}} \quad \frac{0.095}{1.147} \quad 0.08\ \text{s}$$

Second major area

Support plate

The support plate (fig. 6), as part of the reactor core vessel, is the bottom of the volume in which the reactor core components are placed (fuel assemblies, beryllium and aluminum blocks). Its function is to fix axially the core elements during the reactor operation and to provide a reliable passage of the heat carrier from the core to the next element of the internal pool cooling loop. The support plate is represented on fig. 5. Its thickness is 55 mm and the heat carrier passes through the evenly distributed holes.The aluminum blocks cover 12 sockets through which the heat carrier does not pass. These sockets are taken into account and only the section flow areas of 42 slots for elements of the reactor core are practically considered. In the center of each slot along its axis is a circular hole with diameter ø 29 mm, 9 of these holes are with section areas blocked by the I&C system elements, which reduces the number of freeholes to 33.

In the space between them 30 octagonal holes that have more of a square shape with bevels at the corners are placed. The square side is $a = 63.5$ mm and the bevels are with isosceles triangle shape with height to the hypotenuse $h = 18.8$ mm and hypotenuse $b = 37.6$ mm. At each corner the octagon has a curvature with radius $r = 10$ mm. On the periphery of the reactor core 30 holes with shape of divided on the diagonal half octagon are located. At the corners 4 holes with shape of quarter octagon are located.

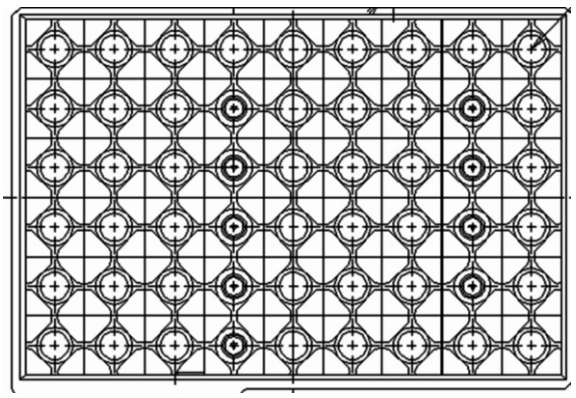

Figure 6. Support plate

To determine the section flow area of the support plate, the sum of the sections flow areas of the holes is calculated. In determining the geometrical dimensions of the octagon, the bevels are not taken into account because their influence to the result is negligible. The geometric parameters of the support plate according to [9] are presented in tab. 4.

According to eq. (7) the heat carrier velocity through the support plate is

$$v_{SP} \quad \frac{v_{RC} S_{RC}}{S_{SP}} \quad \frac{1.147 \ \ 0.054737}{0.142237} \quad 0.441\ \text{m s}^{-1}$$

For the height of the support plate $l_{RC} = 55$ mm according to eq. (8) the decay time in the support plate is

$$t_{SP} \quad \frac{l_{SP}}{v_{SP}} \quad \frac{0.055}{0.441} \quad 0.125\ \text{s}$$

Delay tank

The function of the delay tank is expressed as a sharp reduction of the speed of the heat carrier movement after it exits from the reactor core in order to provide the time for the decay of the short-lived isotopes.This is achieved by a sharp and significant increase in the section flow area of the coolant channel and the change of its movement direction.

The design and the main dimensions of the delay tank according to [9] are presented on fig. 7. The height of the delay tank is 420 mm. At the entrance into the delay tank volume the heat carrier abruptly changes its movement direction at an angle of 90° and enters into the expanding subarea. After the expanding subarea, the heat carrier enters a sharply narrowing section flow area of the throttling baffler.

When considering the heat carrier movement through the delay tank, the following subareas are differentiated:

- the transition of the flow from the support plate to the volume of the delay tank with change of the direction and the section flow area,
- the bilateral expanding subarea,
- the unilaterally expanding subarea, and
- the subarea with a constant cross-section.

Table 4. The geometric parameters of the support plate

Hole	Pcs.	S_n [mm^2]	ΣS_n [mm^2]
29 mm	33	660.19	21786.27
Octagon	30	2618.49	78554.70
½ octagon	30	1309.25	39277.50
¼ octagon	4	654.62	2618.48
S_{SP}	–	–	142236.95

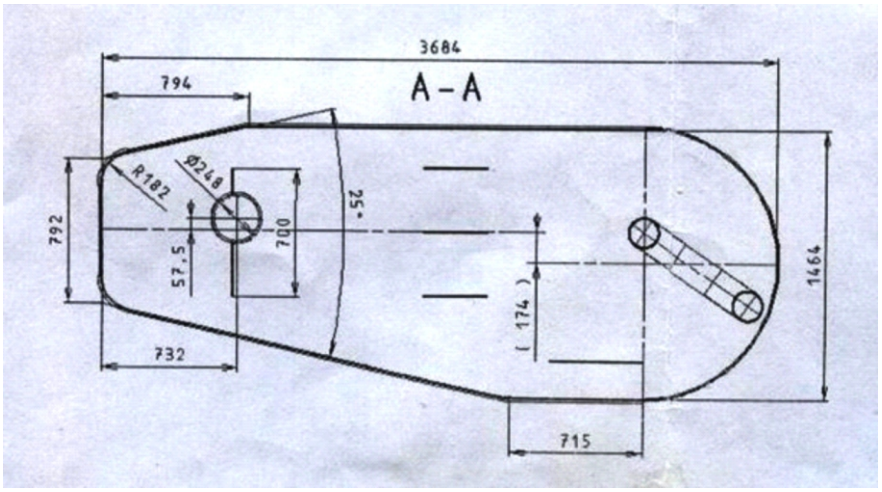

Figure 7. The design and main dimensions of the delay tank (all values are in mm)

Changing the direction of the heat carrier movement and entering the delay tank

The geometric parameters of the transition into the delay tank are width a_{tr} and length b_{tr} of the reactor core, determined by the number of slots through which the heat carrier passes according to [9]:
a_{tr} = 429.0 mm – the width of the reactor core, and
b_{tr} = 500.5 mm – the length of the reactor core.

Then, the section flow area of the transition S_{tr} is

$$S_{tr} \quad a_{tr} b_{tr} \quad 214715\,\text{mm}^2$$

The half of the delay tank height b_{dt} is the average path of the heat carrier transition into the tank at the direction change:
b_{dt} = 420 mm – the height of the delay tank, and
l_{tr} = 210 mm – the average path of the heat carrier transition.

According to eq. (7) the heat carrier velocity of the transition into the delay tank is

$$v_{tr} \quad \frac{v_{SP} S_{SP}}{S_{tr}} \quad \frac{0.441\ 0.142237}{0.214715} \quad 0.292\,\text{ms}^{\ 1}$$

For the average length of the transition l_{tr} = 210 mm according to eq. (8) the transition decay time is

$$t_{tr} \quad \frac{l_{tr}}{v_{tr}} \quad \frac{0.210}{0.292} \quad 0.179\,\text{s}$$

Bilateral expanding subarea

This subarea is a rectangular diffuser section with a symmetric linear extension in one plane, ending with a throttling baffler. The length of the subarea starts from the middle of the reactor core and ends at the throttling baffler. The geometric parameters of the subarea are as follows:
= 25° – the angle of the diffuser expansion, and
$_{ble}$ = 792 mm – the width of the entrance of the diffuser,
b_{bl} = 420 – the height of the diffuser,
l_{bl} = 794 mm – the length of the diffuser subarea,
$a_{blo} = a_{ble} + 2l \tan(\ /2)$ = 1143 mm – the width at the diffuser outlet, and
l_{blp} = 579 mm – the length of the heat carrier average path in the bilateral expanding subarea.

Then the section flow area of the diffuser entrance S_{ble} is

$$S_{ble} = a_{ble} b_{bl} = 332640\ \text{mm}^2$$

According to eq. (7) the heat carrier velocity at the diffuser entrance is

$$v_{ble} \quad \frac{v_{tr} S_{tr}}{S_{ble}} \quad \frac{0.292\ 0.214715}{0.332640} \quad 0.188\ \text{ms}^{\ 1}$$

The section flow area of the diffuser outlet S_{blo} is

$$S_{blo} = a_{blo} b_{bl} = 480060\ \text{mm}^2$$

According to eq. (7) the heat carrier velocity at the diffuser outlet is

$$v_{blo} \quad \frac{v_{ble} S_{ble}}{S_{blo}} \quad \frac{0.188\ 0.332640}{0.480060} \quad 0.130\,\text{ms}^{\ 1}$$

Since the diffuser expansion is linear, the change of the heat carrier velocity also has a linear dependence. Then, the average velocity in the subarea is

$$\overline{v_{bl}} \quad \frac{v_{ble} \quad v_{blo}}{2} \quad 0.159\,\text{ms}^{\ 1}$$

The decay time t_{bl} in the subarea with average velocity $\overline{v_{bl}}$ 0.159 ms ^{1} and length of the heat carrier average path l_{blp} = 543 mm according to eq. (8) is

$$t_{bl} \quad \frac{l_{blp}}{\overline{v_{bl}}} \quad \frac{0.579}{0.159} \quad 3.642\,\text{s}$$

Unilaterally expanding subarea

This subarea is also a diffuser with a rectangular cross-section, but with a unilateral extension in one plane. The geometric parameters of the subarea are as follows:
$\alpha = 12.5^0$ – the angle of the diffuser expansion,
a_{ule} = 1143 mm – the width of the entrance of the diffuser,
b_{ul} = 420 – the height of the diffuser,
l_{ul} = 1443 mm – the length of the diffuser subarea, and

$a_{ulo} = a_{ule} + l \tan(\alpha/2) = 1463$ mm – the width at the diffuser outlet.

The section flow area of the diffuser entrance S_{ule} is

$$S_{ule} = S_{blo} = 480060 \text{ mm}^2$$

The heat carrier velocity at the diffuser entrance is

$$v_{ule} \quad v_{blo} \quad 0.130 \text{ ms}^{1}$$

The section flow area of the diffuser outlet S_{ulo} is

$$S_{ulo} = a_{ulo} b_{ul} = 614460 \text{ mm}^2$$

According to eq. (7) the heat carrier velocity at the diffuser outlet is

$$v_{blo} \quad \frac{v_{ule} S_{ule}}{S_{ulo}} \quad \frac{0.130 \ 0.480060}{0.614460} \quad 0.102 \text{ ms}^{1}$$

Since the diffuser expansion is linear, the change of the heat carrier velocity also has a linear dependence. Then, the average velocity in the subarea is

$$\overline{v_{ul}} \quad \frac{v_{ule} \quad v_{ulo}}{2} \quad 0.116 \text{ ms}^{1}$$

The decay time t_{ul} in the subarea with average velocity $\overline{v_{bl}} \quad 0.116 \text{ ms}^{1}$ and the length of the diffuser subarea $l_{ul} = 1443$ mm according to eq. (8) is

$$t_{ul} \quad \frac{l_{ulp}}{\overline{v_{ul}}} \quad \frac{1.443}{0.116} \quad 12.440 \text{ s}$$

Subarea with a constant cross-section

The subarea with a constant section follows after the diffuser with rectangular cross-section and unilateral extension in one plane. The geometric parameters of the subarea are as follows:

$a_{ccs} = 1463$ mm – the width of the subarea with a constant section,

$b_{ccs} = 420$ mm – the height of the subarea with a constant section, and

$l_{ccs} = 715$ mm – the length of the subarea with a constant section.

Then

$$v_{ccs} = v_{ulo} = 0.102 \text{ ms}^{-1}$$

The decay time t_{ccs} in the subarea with velocity $v_{ccs} = 0.102 \text{ ms}^{-1}$ and the length of the constant section subarea $l_{ccs} = 715$ mm according to eq. (8) is

$$t_{ccs} \quad \frac{l_{ccs}}{v_{ccs}} \quad \frac{0.715}{0.102} \quad 7.010 \text{ s}$$

Here, the heat carrier is a dividing point. From here on, both parts of the heat carrier have different decay time until they reach the unification point. The decay time at the heat carrier dividing point on the second main area t_2 is

$$t_2 \quad t_t \quad t_{SP} \quad t_{tr} \quad t_{bl} \quad t_{ul} \quad t_{ccs} \quad 24.016 \text{ s}$$

Third major area – Part A

From the delay tank, 37 % of the heat carrier debit is sucked by the pump of the primary circulation loop, passes through the heat exchangers and the filter system, and then through a pipeline and the ejector nozzle returns into the internal pool cooling loop.

The flow rate G' through the pump of the primary circulation loop according to [9] is

$$G \quad 37\% G \quad 0.37 \ 226$$
$$83.62 \text{ m}^{-3}\text{h}^{-1} \quad 0.023228 \text{ m}^{-3}\text{s}^{-1}$$

The geometric parameters of the external pool cooling circuit according to [9] and the calculation results according to eq. (5), eq. (7), and eq. (8) are presented in tab. 5.

The decay time in the heat carrier reunification point in the third main area part $A \ t_3^A$ is

$$t_3^A \quad 55.047 \ s$$

The pipes 02-06 and heat exchangers are situated in the premises of the primary circulation loop pump station, where the first control point is also located. The radioactivity of the heat carrier passing through the equipment exerts influence on the radiation situation in the premises. At the inlet of pipe 2 the first control point A is situated, at the outlet of pipe 6 the first control point B is situated.

The summary length of the radiation source is 29.739 m and its volume is 0.429 m^3. The average diameter of the conventional linear source is 0.136 m.

Table 5. Geometric parameters of the external pool cooling circuit and calculation results

Equipment	Diameter [m]	Section [m^2]	Velocity [ms^{-1}]	Length [m]	Passing time [s]
Sucking pipeline	0.203	0.032349	0.718	6.470	9.011
Pipe 01	0.159	0.019846	1.170	14.700	12.564
Pipe 02	0.159	0.019846	1.170	3.940	3.368
Pipe 03	0.089	0.006218	3.734	2.775	0.743
Pipe 04	0.108	0.009156	2.536	6.150	2.425
Heat exchanger	32 0.020	0.010048	2.311	2.821	1.221
Pipe 05	0.108	0.009156	2.536	2.793	1.101
Pipe 06	0.159	0.019846	1.170	11.260	9.624
Pipe 07	0.159	0.019846	1.170	11.110	9.487
Pressure pipe	0.146	0.016733	1.388	7.638	5.503
Summary decay time	–	–	–	–	55.047

Third major area – Part B

From the delay tank 63 % of the heat carrier debit is sucked by the ejector system into the ejector system vessel, passes through the open flow cross-section at the ejector system entrance between the internal surface of the ejector system sucking pipe and external surface of the ejector nozzle pressure pipe and surrounds the nozzle. The ejector system plan is represented on fig. 7.

The flow rate G'' through the open flow cross-section at the ejector system entrance according to [9] is

$$G \quad 63\%G \quad 0.63 \quad 226$$

$$142.38 \text{ m}^3\text{h}^{-1} \quad 0.039550 \text{ m}^3\text{s}^{-1}$$

The internal diameter of the ejector system sucking pipe is D_{SP} = 381.4 mm, the external diameter of the ejector nozzle pressure pipe is D_{NPP} = 229.0 mm, and the length of the ejector system entrance is l_{ese} = = 270 mm.

Then the open flow area of the ejector system entrance S_{ese} is

$$S_{ese} \quad \frac{\pi D_{SP}^2}{4} \quad \frac{\pi D_{NPP}^2}{4} \quad \frac{\pi (D_{SP}^2 - D_{NPP}^2)}{4}$$

$$\frac{3.14 \quad (0.145466 \quad 0.052441)}{4}$$

$$S_{ese} = 0.073062 \text{ m}^2$$

According to eq. (5) with such a debit the heat carrier velocity v_{ese} is

$$v_{ese} \quad \frac{G}{S_{ese}} \quad \frac{0.039550}{0.073062} \quad 0.541 \text{ ms}^{-1}$$

The decay time t_{ese} in the subarea with velocity v_{ese} = 0.541 ms^{-1} and the length of the ejector system entrance l_{ese} = 270 mm according to eq. (8) is

$$t_{ese} \quad \frac{l_{ese}}{v_{ese}} \quad \frac{0.270}{0.541} \quad 0.499 \text{ s}$$

The decay time at the heat carrier reunification point in the third main area part B t_3^B is

$$t_3^B \quad 0.499 \text{ s}$$

Fourth major area

At the ejector nozzle both heat carrier streams are reunited and mixed. Before reaching the grid of the ejector system vessel, the heat carrier passes through the ejector (fig. 8), changes its movement direction at the angle of 180°, and at the grid again changes its movement direction at the angle of 90° and passes through the grid (a decay time area).

The above described heat carrier path through the ejector system is divided into the following subareas:

– the first subarea: a confusor section, a section with a constant diameter and a diffuser section,

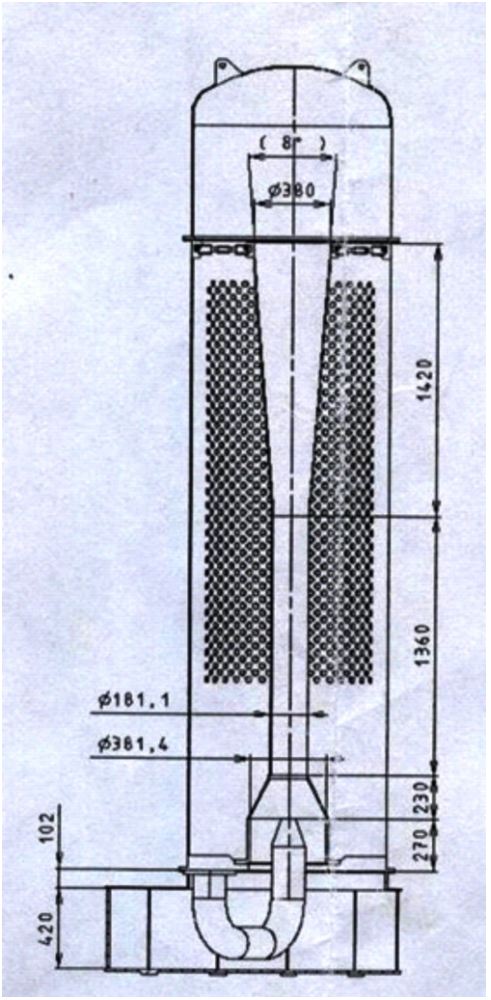

Figure 8. Ejector system (all values are in mm)

– the second subarea where the movement direction reverses within the housing of the ejector system, and
– the third subarea in which the grid mid-height of the ejector system vessel is reached and the heat carrier exits laterally from the vessel of the ejector system through the vessel grid.

First subarea: a confusor section, a section with a constant diameter and a diffuser section

From the delay tank and the pump station of the primary external cooling circuit both parts of the heat carrier are reunited at the confusor entrance. The heat carrier stream passes through the open flow cross-section at the confusor entrance (fig. 9). The internal diameter of the confusor entrance is D_{ce} = 381.4 mm.

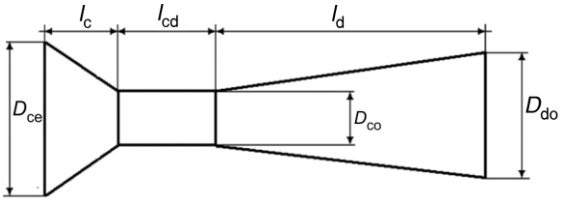

Figure 9. Confusor-diffuser areas

Then, the open flow area of the confusor entrance S_{ce} is

$$S_{ce} \quad \frac{\pi D_{ce}^2}{4} \quad \frac{3.14 \ 0.145466}{4} \quad 0.114249\,\mathrm{m}^2$$

At the confusor entrance, the heat carrier debit is equal to the debit at the dividing point and according to eq. (5) the heat carrier velocity at the confusor entrance v_{ce} is

$$v_{ce} \quad \frac{G}{S_{ce}} \quad \frac{0.062778}{0.114249} \quad 0.549\,\mathrm{ms}^{-1}$$

The internal diameter of the confusor outlet is D_{co} = 181.1 mm. The open flow area of the confusor outlet S_{co} is

$$S_{co} \quad \frac{\pi D_{co}^2}{4} \quad 0.025759\,\mathrm{m}^2$$

According to eq. (7) the heat carrier velocity at the confusor outlet is

$$v_{co} \quad \frac{v_{ce} S_{ce}}{S_{co}} \quad \frac{0.549 \ 0.114249}{0.025759} \quad 2.435\,\mathrm{ms}^{-1}$$

Since the confusor expansion is linear, the change of the heat carrier velocity also has a linear dependence. Then, the average velocity in the confusor section is

$$\overline{v}_c \quad \frac{v_{ce} \quad v_{co}}{2} \quad 1.492\,\mathrm{ms}^{-1}$$

The decay time t_c in the confusor section with velocity $\overline{v}_c$ 1.492 ms^{-1} and length of the ejector system confusor l_c = 232 mm according to eq. (8) is

$$t_c \quad \frac{l_c}{\overline{v}_c} \quad \frac{0.232}{1.492} \quad 0.155\ \mathrm{s}$$

The internal diameter of the section with a constant diameter is equal to the confusor outlet diameter $D_{cd} = D_{co}$ = 181.1 mm. In this case

$$S_{cd} \quad S_{co} \quad 0.025759\,\mathrm{m}^2$$

and

$$v_{cd} \quad v_{co} \quad 2.435\,\mathrm{ms}^{-1}$$

The decay time t_{cd} in the section with a constant diameter with the velocity v_{cd} = 1.492 ms^{-1} and the length l_{cd} = 1360 mm according to eq. (8) is

$$t_{cd} \quad \frac{l_{cd}}{v_{cd}} \quad \frac{1.360}{2.435} \quad 0.559\ \mathrm{s}$$

The internal diameter of the diffuser entrance is equal to the diameter of the section with a constant diameter $D_{de} = D_{cd}$ = 181.1 mm. In this case

$$S_{de} \quad S_{cd} \quad 0.025759\,\mathrm{m}^2$$

and

$$v_{de} \quad v_{cd} \quad 2.435\,\mathrm{ms}^{-1}$$

The internal diameter of the diffuser outlet is D_{do} = 380.0 mm. The open flow area of the diffuser outlet S_{do} is

$$S_{do} \quad \frac{\pi D_{do}^2}{4} \quad 0.0113411\,\mathrm{m}^2$$

According to eq. (7) the heat carrier velocity at the diffuser outlet is

$$v_{do} \quad \frac{v_{de} S_{de}}{S_{do}} \quad \frac{2.435 \ 0.025759}{0.113411} \quad 0.553\,\mathrm{ms}^{-1}$$

Since the diffuser expansion is linear, the change of the heat carrier velocity also has a linear dependence. Then, the average velocity in the diffuser section is

$$\overline{v_d} \quad \frac{v_{de} \quad v_{do}}{2} \quad 1.494\,\mathrm{ms}^{-1}$$

The decay time t_d in the diffuser section with velocity $\overline{v_d}$ 1.494 ms^{-1} and the length of the ejector system diffuser l_d = 1420 mm according to eq. (8) is

$$t_d \quad \frac{l_d}{\overline{v_d}} \quad \frac{1.420}{1.494} \quad 0.952\ \mathrm{s}$$

The decay time in the first subarea which consists of the confusor section, the section with a constant diameter and the diffuser section is

$$t_4^1 \quad t_c \quad t_{cd} \quad t_d \quad 1.666\,\mathrm{s}$$

Subarea where the movement direction reverses within the housing of the ejector system

In this subarea the heat carrier exits from the diffuser, penetrates into the volume of the ejector system housing and reverses its movement direction at the angle of 180°. The parameters of the area are as follows (fig. 10):

D_{do} = 380.0 mm – the internal diameter of the diffuser outlet,

D_{esh} = 1006.0 mm – the internal diameter of the ejector system housing,

h = 901.0 mm – the distance between the diffuser outlet and the wall of the ejector system housing,

$l_{esh} = 2\,h$ = 1802.0 mm – the length of the heat carrier path,

v_{do} = 0.553 ms^{-1} – the heat carrier velocity at the diffuser outlet, and

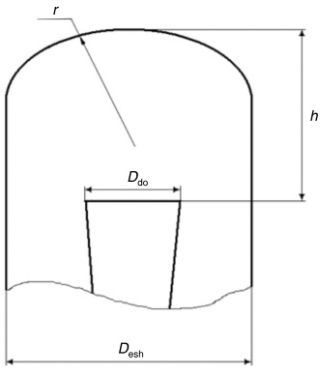

Figure 10. Diffuser outlet and ejector system housing

$S_{do} = 0.113411$ m^2 – the open flow area of the diffuser outlet.

The open flow area of the ejector system housing S_{esh} is

$$S_{esh} \quad \frac{\pi D_{esh}^2}{4} \quad 0.794851 \text{ m}^2$$

According to eq. (7) the heat carrier velocity at the diffuser outlet is

$$v_{esh} \quad \frac{v_{do} S_{do}}{S_{esh}} \quad \frac{0.553 \quad 0.113411}{0.794851} \quad 0.079 \text{ ms}^{-1}$$

The decay time t_{esh} in the ejector system housing section with the velocity $v_{esh} = 0.079$ ms^{-1} and the length of the heat carrier path $l_{esh} = 1802.0$ mm according to eq. (8) is

$$t_{esh} \quad \frac{l_{esh}}{v_{esh}} \quad \frac{1.802}{0.079} \quad 22.810 \text{ s}$$

The decay time in the second subarea where the movement direction reverses within the housing of the ejector system is

$$t_4^2 \quad 22.810 \text{ s}$$

Subarea in which the grid mid-height of the ejector system vessel is reached and the heat carrier exits laterally from the vessel of the ejector system through the vessel grid

In this subarea the heat carrier passes through the open flow cross section between the internal surface of the ejector system housing and the external surface of the ejector diffuser. From the ejector diffuser outlet to the entrance level of the ejector the diffuser (the grid mid-height) exits laterally from the vessel of the ejector system at an angle of 90º through the vessel grid.

When considering this subarea of the internal pool circulation loop (fig. 11), there are two distinct sections:

– the heat carrier movement in the housing of the ejector system to the entrance level of the ejector diffuserm, and
– the lateral exit from the vessel of the ejector system at an angle of 90° through the vessel grid.

The geometrical parameters of the first section are as follows:

$D_{do} =$ 390.0 mm – the external diameter of the diffuser outlet,

$D_{de} =$ 191.1 mm – the external diameter of the diffuser entrance,

$D_{esh} =$ 1006.0 mm – the internal diameter of the ejector system housing, and

$l_d =$ 1420.0 mm – the length of the ejector system diffuser.

The open flow area between the internal surface of the ejector system housing and the external surface of the ejector diffuser outlet S_1 is

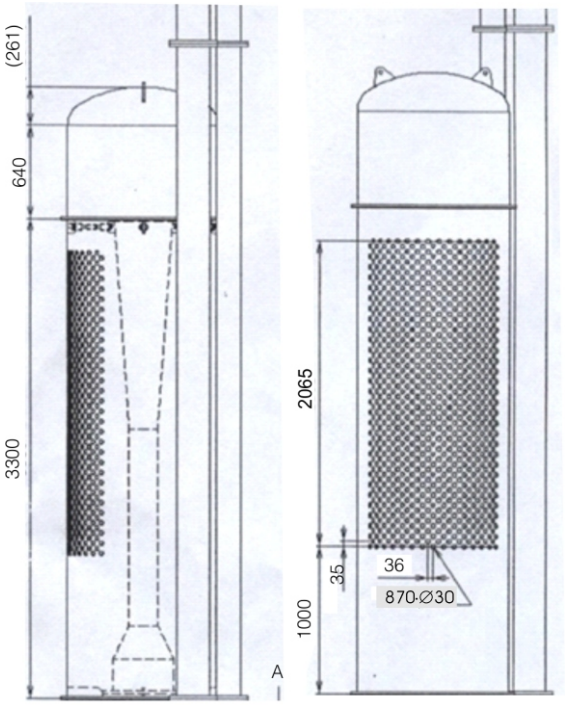

Figure 11. Grid of the ejector system vessel (all values are in mm)

$$S_1 \quad \frac{\pi D_{esh}^2}{4} \quad \frac{\pi D_{do}^2}{4} \quad \frac{\pi (D_{esh}^2 \quad D_{do}^2)}{4}$$

$$\frac{3.14 \quad (1.012036 \quad 0.152100)}{4}$$

$$S_1 \quad 0.675392 \text{ m}^2$$

The open flow area between the internal surface of the ejector system housing and the external surface of the ejector diffuser entrance S_2 is

$$S_2 \quad \frac{\pi D_{esh}^2}{4} \quad \frac{\pi D_{de}^2}{4} \quad \frac{\pi (D_{esh}^2 \quad D_{de}^2)}{4}$$

$$\frac{3.14 \quad (1.012036 \quad 0.036519)}{4}$$

$$S_2 \quad 0.766169 \text{ m}^2$$

According to eq. (5) the heat carrier velocity in the ejector system housing at the outlet level of the ejector diffuser v_1 is

$$v_1 \quad \frac{G}{S_1} \quad \frac{0.062778}{0.675392} \quad 0.093 \text{ ms}^{-1}$$

According to eq. (7) the heat carrier velocity at the outlet level of the ejector diffuser v_2 is

$$v_2 \quad \frac{v_1 S_1}{S_2} \quad \frac{0.093 \quad 0.675392}{0.766169} \quad 0.082 \text{ ms}^{-1}$$

Since the open flow area expansion is linear, the change of the heat carrier velocity also has a linear dependence. Then, the average velocity in the first section is

$$\overline{v_{fs}} \quad \frac{v_1 \quad v_2}{2} \quad 0.088 \text{ ms}^{-1}$$

The decay time t_{fs} in the first section with the velocity $\overline{v_{fs}}$ 0.088 ms^{-1} and the length of the ejector system diffuser $l_d = 1420$ mm according to eq. (8) is

$$t_{fs} \quad \frac{l_d}{v_{fs}} \quad \frac{1.420}{0.088} \quad 16.136 \text{ s}$$

The geometrical parameters of the second section (fig. 10) are as follows:
$d_g =$ 30.0 mm – the diameter of the grid holes,
$l_g = 8.0$ mm – the wall thickness of the ejector system vessel,
$N_{gh} = 870$ – the number of the grid holes, and
$l_{ss} = l_g + D_{esh}/2$ – the length of the average heat carrier path in the second section.

The open flow area of the grid holes of the ejector system housing $S_{\Sigma gh}$ is

$$S_{\Sigma gh} \quad N_{gh}\frac{\pi d_g^2}{4} \quad 870\frac{3.14 \quad 0.03^2}{4} \quad 0.614967 \text{ m s}^{-1}$$

According to eq. (5), the heat carrier velocity in the second section is equal to the heat carrier velocity in the grid holes of the ejector system housing v_{gh}

$$v_{ss} \quad v_{gh} \quad \frac{G}{S_{\Sigma gh}} \quad \frac{0.062778}{0.614967} \quad 0.102 \text{ m s}^{-1}$$

The average heat carrier path in the second section is

$$l_{ss} \quad l_g \quad \frac{D_{esh}}{2} \quad 8 \quad \frac{1006.0}{2} \quad 511 \text{ mm}$$

The decay time t_{ss} in second section with the velocity $v_{ss} = 0.102$ ms^{-1} and the length of the average heat carrier path $l_{ss} = 511$ mm according to eq. (8) is

$$t_{ss} \quad \frac{l_{ss}}{v_{ss}} \quad \frac{0.511}{0.102} \quad 5.010 \text{ s}$$

The decay time in the third subarea in which the grid mid-height of the ejector system vessel is reached and the heat carrier exits laterally from the vessel of the ejector system through the vessel grid is

$$t_4^3 \quad t_{fs} \quad t_{ss} \quad 21.146 \text{ s}$$

The decay time in the fourth main area t_4 is

$$t_4 \quad t_4^1 \quad t_4^2 \quad t_4^3 \quad 45.146 \text{ s}$$

Fifth major area

From the grid of the ejector system vessel the heat carrier flow penetrates into the pool volume, wherein the flow is mixed with the water in the pool (the decay time area). Based on the preliminary assumptions the heat carrier flow penetrates into the pool volume, wherein the flow traverses to a larger cross-section, moves horizontally to the point situated above the reactor core center, descends vertically to the entrance of the reactor core and penetrates into it.

The grid height h_{pv} and the pool width b_{pv} are assumed as the dimensions of the larger cross-section

$$h_{pv} \quad 2065 \text{ mm}$$

$$b_{pv} \quad 1800 \text{ mm}$$

The length of the heat carrier path through the pool volume to the reactor core inlet is the sum of horizontal l_{hpv} and vertical l_{vpv} parts

$$l_{hpv} \quad 2605 \text{ mm}$$

$$l_{vpv} \quad 2664 \text{ mm}$$

$$l_{pv} \quad 2605 \quad 664 \quad 3269 \text{ mm}$$

The open flow area of the larger cross-section in the pool volume S_{pv} is

$$S_{pv} \quad h_{pv}\, b_{pv} \quad 2.065 \quad 1.800 \quad 3.717 \text{ m}^2$$

According to eq. (7) the heat carrier velocity through the pool volume v_{pv} is

$$v_{pv} \quad \frac{v_{gh}\, S_{\Sigma gh}}{S_{pv}} \quad \frac{0.102 \quad 0.614967}{3.717} \quad 0.017 \text{ m s}^{-1}$$

The decay time t_{hpv} in the pool volume at the control point 2-B with the velocity $v_{pv} = 0.017$ ms^{-1} and the length of the heat carrier path through the pool volume $l_{hpv} = 2605$ mm according to eq. (8) is

$$t_{hpv} \quad \frac{l_{hpv}}{v_{pv}} \quad \frac{2.605}{0.017} \quad 153.235 \text{ s}$$

The decay time t_{pv} in the pool volume with the velocity $v_{pv} = 0.017$ ms^{-1} and the length of the heat carrier path through the pool volume $l_{pv} = 3269$ mm according to eq. (8) is

$$t_{pv} \quad \frac{l_{pv}}{v_{pv}} \quad \frac{3.269}{0.017} \quad 192.294 \text{ s}$$

In the second control point a radiation source with the volume of 9.6828 m^3 is situated.

CALCULATION RESULTS

The summary calculation results of the irradiation duration (ID) and the decay time (DT) in the dividing point (DP), the control points (CP), at the reactor core inlet (RCI) and the cycle duration (CD) are presented in tab. 6.

Table 6. The summary results of the irradiation duration and the decay time calculations

Flow rate [%]	ID [s]	Decay time in DP [s]	Decay time in CP 1-A [s]	Decay time in CP 1-B [s]	Decay time in CP 2-A [s]	Decay time in CP 2-B [s]	Decay time at RCI [s]	CD [s]
100	0.540	24.096	–	–	–	–	–	–
37	–	–	45.671	64.153	124.289	277.524	316.583	317.123
63	–	–	–	–	69.741	222.976	262.035	262.575

Based on the preliminary assumptions about the heat carrier pressure and the temperature in all of the major areas, the properties of the heat carrier are equal.

The average temperature and pressure of the heat carrier in the reactor core are

$$T_{RC}^{0} \quad 47.26 \quad C$$

$$P_{RC} \quad 0.1499\ MPa$$

At this temperature and pressure the heat carrier density according to [12] is

$$\gamma \quad 989.2515\ kgm^{3} \quad 0.9892515\ gcm^{3}$$

At such heat carrier properties the nuclear density, the macroscopic cross-section of the activation and the integral of the activation of the observed isotopes predecessors are presented in tab. 7.

The calculation results of the circulation cycle numbers (CCN) after which the concentration equilibrium is observed for every isotope and for every branch of the heat carrier are presented in tab. 8.

The calculation results of the separate and the summary isotope specific activity in the control points and at the reactor core inlet after the concentration equilibrium is achieved are presented in tab. 9.

The geometrical shape and dimensions (GSD) of the technological radiation sources, the average specific activity (ASA) of the neutron and the gamma-particle radiation source, the particles type and energy (PTE) in the control points are presented in tab. 10.

Based on the calculation results, the influence of the technological radiation sources on the radiation situation in the control points could be assessed.

DISCUSSIONS

It is known that after the ten half-life periods, approximately 0.1 % of the initial amount of the radioactive nuclei remains. If this value is considered to be negligible on the basis of the presented data in tab. 2 and tab. 6, it could be expected that the concentration of the isotopes ^{16}N and ^{17}N is zero at the beginning of

Table 7. The nuclear density, the macroscopic cross-section of activation, and the integral of activation of the observed isotopes predecessors

Nuclide predecessor	Nuclear density [10^{-24} cm^{-3}]	Reaction of the activation	Macroscopic cross-section of the reaction [10^{6} cm^{-1}]	Integral of the activation [10^{-7} cm^{-3}s^{-1}]
^{16}O	0.032989	^{16}O (n , p) ^{16}N	0.626791	0.871866
^{17}O	0.000013	^{17}O (n , p) ^{17}N	0.000069	0.000096
^{18}O	0.000066	^{18}O (n , p) ^{18}F	0.000528	0.000734
^{18}O	0.000066	^{18}O (n ,) ^{19}O	0.000106	0.000147

Table 8. The calculation results of the circulation cycle numbers after which the concentration equilibrium is observed for every isotope and for every branch of the heat carrier

Flow rate [%]	Isotope	CP 1-A, CCN	CP 1-B, CCN	CP 2-A, CCN	CP 2-B, CCN	RCI, CCN
37	^{16}N	1	1	1	1	1
37	^{17}N	1	1	1	1	1
37	^{18}F	302	431	182	168	154
37	^{19}O	2	2	2	2	2
63	^{16}N	–	–	1	1	1
63	^{17}N	–	–	1	1	1
63	^{18}F	–	–	219	256	232

Table 9. The calculation results of the separate and the summary activity of the isotopes in the control points and at the reactor core inlet

Flow rate [%]	Isotope	CP 1-A [Bqcm^{-3}]	CP 1-B [Bqcm^{-3}]	CP 2-A [Bqcm^{-3}]	CP 2-B [Bqcm^{-3}]	RCI [Bqcm^{-3}]
37	^{16}N	5263.9400	873.2989	2.5278	0.0000	0.0000
37	^{17}N	0.0397	0.0018	0.0000	0.0000	0.000
37	^{18}F	12.6470	12.6225	0.0171	0.0168	0.0167
37	^{19}O	6.2639	3.8917	0.8271	0.0159	0.0058
63	^{16}N	–	–	507.3254	0.0002	0.0000
63	^{17}N	–	–	0.0007	0.0000	0.0000
63	^{18}F	–	–	0.0205	0.0205	0.0203
63	^{19}O	–	–	3.3730	0.0652	0.0238
100	^{16}N	5263.9400	873.2989	320.5503	0.0002	0.0000
100	^{17}N	0.0397	0.0018	0.0007	0.0000	0.0000
100	^{18}F	12.6470	12.6225	0.0192	0.0191	0.0190
100	^{19}O	6.2639	3.8917	2.4310	0.0470	0.0171

Table 10. The calculation results of the properties of the technological radiation sources in the control points

GSD [m]	Isotope	ASA [Bqcm^{-3}]	PTE [MeV]
CP-1, tubular linear source, 0.136×29.739	^{16}N	3068.6195	γ, 6.13
	^{17}N	0.0208	*n*, 1.60
	^{18}F	12.6348	γ, 1.40
	^{19}O	5.0778	γ, 1.20
CP-2, parallelepiped volume source, 1.800 2.065 2.605	^{16}N	160.2753	γ, 6.13
	^{17}N	0.0004	n, 1.60
	^{18}F	0.0192	γ, 1.40
	^{19}O	1.2390	γ, 1.20

each heat carrier circulation cycle, as evidenced by the calculations.

According to the evaluation results, the concentration equilibrium of the oxygen isotope ^{19}O occurs in all control points in the circulation cycle number $k = 2$.

Due to the significantly longer half-life period of the fluorine isotope ^{18}F than the duration of the circulation cycle, its concentration in the control points increases until a balance between the accumulation and the decay is achieved. The number of necessary cycles for occurrence of this equilibrium is different for every control point and heat carrier branch. The maximum circulation cycle number $k = 431$ for a cycle duration of approximately 317 seconds means about 38 hours of uninterrupted operation of the facility. Most research reactors, especially those with a rated power of 2 MW or less, are operated in a cyclic mode. This means the operation of about 8 hours and staying about 16 hours per day during the five working days of the week and staying through the weekend. For a detailed analysis, the operation mode should be taken into account.

CONCLUSIONS

Due to the delay tank presence in the design, the heat carrier velocity slows down sharply after the reactor core. This provides a heat carrier run duration in CP-1A of more than six half-life periods of the isotope ^{16}N, whose predecessor ^{16}O has the highest content (99.7 %) in the heat carrier and more than ten half-life periods of the isotope ^{17}N, which radiates neutrons in the decay process. This significantly reduces the activity of the technological radiation sources in the pumping station of the primary circulation loop.

ACKNOWLEDGEMENTS

This work is devoted to honoring the memory of Professor Natalia Janeva, Ph. D., D. Sc., from the Institute for Nuclear Research and Nuclear Energy, Bulgarian Academy of Science, Sofia, Bulgaria, European Union, for her valuable assistance in the work on training of young specialists in the sphere of theoretical and experimental neutron, nuclear, and reactor physics, nuclear energy and nuclear technology, and the memory of Prof. Pavel Egorenkov from the RRC "Kurchatov Institute", Moscow, Russian Federation, for his valuable assistance in the work on the reconstruction of the research reactor in Sofia.

REFERENCES

[1] Perevezentsev, V. V., Processes of Transference and Accumulation of Activity in the Technological Loop of Nuclear Power Plant (in Russian), Publishing house of MSTU Bauman, Moscow, 2004
[2] ***, IAEA-TECDOC-825, Reference and Intercomparison Materials for Stable Isotopes of Light Elements, *Proceedings*, Consultants Meeting Held in Vienna, December 1-3, 1993
[3] Golubev, B. P., Dosimetry and Protection from Ionizing Radiation (in Russian), Atomizdat, Moscow, 1976
[4] Egorov, J. A., Radiation Safety Basics of NPP, Energoizdat (in Russian), Moscow, 1982
[5] Nesmeyanov, A. N., *et al*., Production of Radioactive Isotopes (in Russian), State Scientific and Technical Publishing House of the Chemical Literature, Moscow, 1954
[6] Gusev, N. G., *et al*., Protection from Ionizing Radiation (in Russian), Vol. 2, Ergoatomizdat, Moscow, 1990
[7] Idelchik, I. E., Handbook of Hydraulic Resistances (in Russian), 3^{ed} ed., Mashinostroenie, Moscow, 1992
[8] Kadalev, S., Safety Analysis Method in Case of Black-Out Accident on Pool Type Research Reactor, *Progress in Nuclear Energy, 78* (2015), Jan., pp. 121-135
[9] ***, Technical Design for the Reconstruction of the IRT-2000 Reactor at INRNE BAS to Low-Power Reactor (in Bulgarian), INTERATOM, Sofia, 2003
[10] ***, "B 0019.20.00.000 DKO Fuel Assemblies IRT-4M Catalogue Description (in Russian), NZHK, 2008
[11] Samoylov, O. B., *et al.*, Safety of Nuclear Power Plants, Ergoatomizdat (in Russian), Moscow, 1989
[12] Rivkin, S. L., Alexandrov, A. A., Thermodynamic Properties of the Water and the Water Vapor (in Russian), Ergoatomizdat, Moscow, 1984

Received on April 3, 2017
Accepted on December 13, 2017

Стојан Х. КАДАЛЕВ

ПРОЦЕНА ТЕХНОЛОШКИХ РАДИОАКТИВНИХ ИЗВОРА У ПУМПНОЈ СТАНИЦИ ПРИМАРНЕ ЦИРКУЛАЦИОНЕ ПЕТЉЕ И НА ВРХУ ИСТРАЖИВАЧКОГ РЕАКТОРА БАЗЕНСКОГ ТИПА

У овом раду разматра се процена технолошких радиоактивних извора у примарној вода-вода циркулационој петљи реактора. У принципу, оваква процена је мултидисциплинарни задатак који узима у обзир не само озрачивање језгра, формирање нових изотопа и њихов распад уколико су нестабилни, већ и прорачуне у области хидраулике ради процене времена озрачивања и времена распада. Приказан је како општи тако и детаљнији преглед настанка радиоактивних извора у нуклерним постројењима и истраживачким реакторима базенског типа са деминерализованом водом као топлотним носиоцем. Почетни изотопски састав топлотног носиоца усвојен је према Бечком стандарду просечне океанске воде предложеном од Међународне агенције за атомску енергију. Детаљно је описан општи математички модел процеса озрачивања језгра, настанка нових изотопа и њиховог распада, дата је оцена времена озрачивања и времена распада, чиме је омогућено понављање ове процене у одређеном постројењу. Приказана метода примењена је у пројекту реконструкције нуклеарног истраживачког реактора IRT-2000 у Софији, Бугарска.

Кључне речи: индуковано зрачење, активација топлотног носиоца, технолошки радиоактивни извор